



# **Design and Construction of a System for Measuring Carbon Monoxide, Hydrogen and Methane Concentrations in a Co-Current Downdraft Biomass Gasifier**

**Zoundi Ousmane <sup>a\*</sup>, Nzihou Jean Fidele <sup>a</sup>, Hamidou Salou <sup>b</sup>, Ouattara Frederic <sup>a</sup> and Segda Bila Gerard <sup>c</sup>**

<sup>a</sup> *Analytical Chemistry, Spatial Physics and Energetic Laboratory, Norbert Zongo University, Koudougou, Burkina Faso.*

<sup>b</sup> *Catholic University of West Africa, University Unit in Bobo-Dioulasso, Bobo-Dioulasso, Burkina Faso.*

<sup>c</sup> *Environnemental Physic and Chemistry Laboratory, Joseph Ki-Zerbo University, Ouagadougou, Burkina Faso.*

## **Authors' contributions**

*This work was carried out in collaboration among all authors. All authors read and approved the final manuscript.*

## **Article Information**

DOI: 10.9734/CJAST/2024/v43i24353

## **Open Peer Review History:**

This journal follows the Advanced Open Peer Review policy. Identity of the Reviewers, Editor(s) and additional Reviewers, peer review comments, different versions of the manuscript, comments of the editors, etc are available here: <https://www.sdiarticle5.com/review-history/112774>

**Original Research Article**

**Received: 28/11/2023**

**Accepted: 03/02/2024**

**Published: 08/02/2024**

## **ABSTRACT**

Gasification is the process of producing combustible gases from solid materials such as coal, biomass or solid waste. The laboratory of Space Physics and Energy has two experimental gasifiers producing synthetic gases whose natures and concentrations must be determined. To do this, lower-cost sensors were purchased and used for determining the concentration of carbon monoxide

\*Corresponding author: E-mail: zounous@gmail.com;

with maximum concentration of 1.000 and 2.000 ppm. Hydrogen and methane concentration was not offered by these two commercial gas analyzers. In this paper Metal-Oxide gas sensors were used to extend the measurement range of carbon monoxide up to 4.000ppm. Hydrogen and methane concentrations up to 10.000ppm in synthetic gas produced by a wood fired co-current downdraft gasifier measurements were also enabled. These sensors have a chemical sensing element based on a layer of tin dioxide ( $\text{SnO}_2$ ); whose resistivity is sensitive to nature of the gas between two sensing electrodes. This property gives these sensors a resistive electrical model whose measurand is the concentration of the input gas. This study shows that resistor R of the sensor is related to the gas concentration with an equation of the form:  $\log(R/R_0) = A \log(x) + B$ . With  $A = -0.3072$ ,  $B = 0.921$  for methane,  $A = -0.6527$ ,  $B = 1.3055$  for carbon dioxide and  $A = -1.522$ ,  $B = 4.5686$  for hydrogen.

**Keywords:** Gasification; modelling; concentration; carbon monoxide; hydrogen; methane.

## 1. INTRODUCTION

Burkina Faso, efforts to reduce energy dependence (of populations and industries on fossil resources and wood) are being carried out through the development of renewable energy sources such as photovoltaic and thermal solar [1,2]. To make our contribution to this concern, the Laboratory has therefore embarked on the construction of experimental gasifiers producing synthetic gases usable for the production of electricity. From May to August 2022, a first downdraft gasifier was designed and successfully tested two wood fired downdraft biomass in Burkina Faso [3,4]. A second gasifier was designed and built from September to December 2022 in order to overcome design flaw that was found in the first gasifier during the testing's. The two gasifiers built are of the co-current type which are already used in industry from 100kW and above for their suitability, as well as their relative ease of manufacturing in developing countries.

Biomass gasification produce a synthesis gas mainly consisting of combustibles gases such as carbon monoxide, hydrogen and small amount of methane and incombustibles gases like nitrogen of the air, carbon dioxide and water vapor [5-9].

The two gasifiers used commercial flue gas analyzers for measuring the produced gases concentrations. But only carbon monoxide with a maximum concentration of 1000 and 2000 ppm where was available. None of the available gas analyzers offered hydrogen and methane concentration measurement.

As said by Yulin Kong et al. [10]: " $\text{SnO}_2$  has been extensively used in the detection of various gases. As a gas sensing material,  $\text{SnO}_2$  has excellent physical-chemical properties, high reliability, and short adsorption-desorption time". It was also found in the literature that other authors were already using cheap gas monitoring sensors for industrial applications [11,12,13]. It was also found that a microcontroller can be used to acquire data from numerous sensors, compute several mathematical functions and display these values [14,15,16]. This is why it was anticipated that the combination of these gas sensors with a microcontroller constitute a cost-effective solution for monitoring gas concentrations in our biomass gasifiers and decided to build an experimental prototype system for measuring these gases, in particular carbon monoxide, hydrogen and methane.

## 2. MATERIALS AND METHODS

### 2.1 Experimental setup

The gasifier used in this work is composed of several functional units:

- The reactor
- The cyclone
- The condenser
- The filter

Fig. 1 shows the overview of these different parts. MQ gas sensors are located on a sampling box that draw small amount of synthetic gas cleaned of tar and water vapor by the cyclone separator, the condenser and the filter.

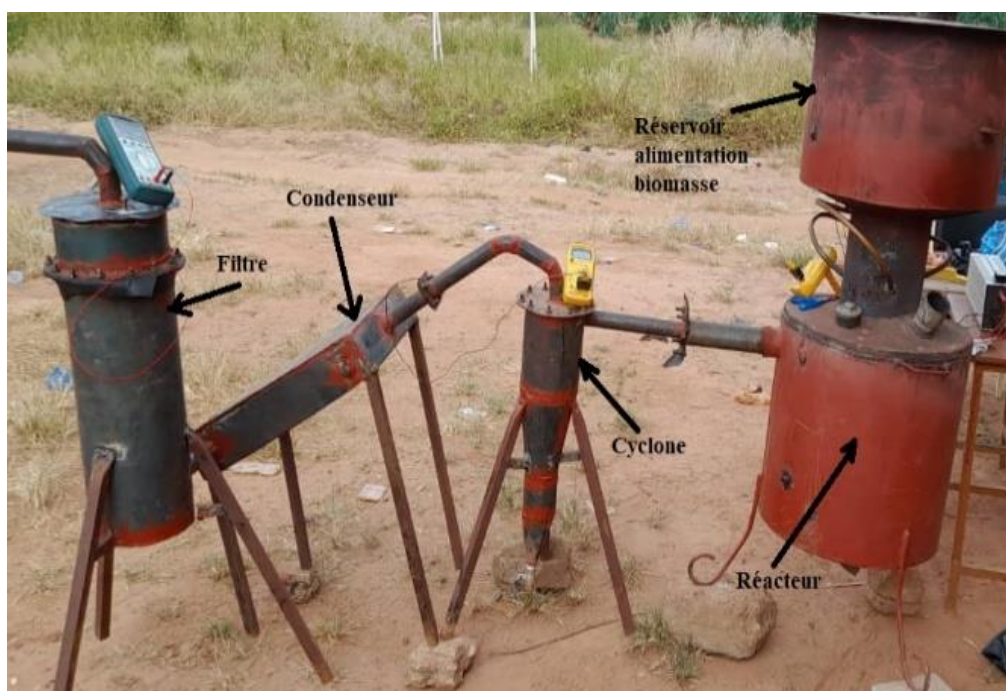


Fig. 1. Experimental setup

## 2.2 Methods

The main gases whose concentrations we want to detect and measure are: H<sub>2</sub>, CO and CH<sub>4</sub>. the respective sensors are: MQ-8, MQ-7, MQ-4.

### 2.2.1 Chemical behaviour of MQ gas sensors

The basic chemical element of MQ gas sensors is a tin dioxide (SnO<sub>2</sub>) layer. From an electrical point of view, a perfect SnO<sub>2</sub> crystal exhibits insulating behavior, due to its wide bandgap. Depending on the purity of the material, we note in the literature a large dispersion of the experimental values of the bandgap which varies between 2.25 to 4.3 eV [17]. On the basis of the results obtained by Jacquemin [18], we can consider that the band gap is direct and that the value of this band gap at room temperature varies between 3.5 to 4 eV. At the opposite, the real crystal has a semiconductor character. This behavior results from deviations from stoichiometry and is closely linked to the presence of oxygen vacancies leading to the presence of donor-type energy levels inside the bandgap [19].

### 2.2.2 Operating principle

The electrical properties of tin oxide layers are species on the surface of the layer modifies its

conductivity by a modification of the electronic states of the semiconductor by movement of electrons from the valence band towards the conduction band. This process is done in three steps [11].

Firstly, the layer is brought into contact with air and the adsorption of dioxygen molecules causes their dissociation and ionization in O<sup>-</sup> form (the most stable species at high temperature) by tearing off an electron from the band. conduction of the layer. Secondly, the reducing gas molecules, to be detected, react on the surface with the anions releasing an electron towards the conduction layer of the oxide and varying its electrical conductivity depending on the number of active oxidation sites and the number of gas molecules chemisorbed on the surface. Thirdly, following the cessation of the introduction of the gas, the oxygen present in the atmosphere adsorbs again on the surface of the oxide, returning to the equilibrium state established during the first process. However, this return to the equilibrium state assumes the absence of phenomena of poisoning of the sites by secondary molecules resulting from oxidation reactions [12].

Given the above, the resistivity of the tin oxide layer varies depending on the concentration of

environmental gases. We can model it by a variable resistance depending on the concentrations as shown on Fig. 2.

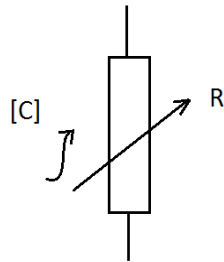


**Fig. 2. Electrical model of a MQ gas sensor**

**2.2.3 Presentation of the sensors**

The following Fig. 3 is the representation of a gas MQ sensors.

Each SnO<sub>2</sub> sensor is composed of the elements in Table 1 below:

**Table 1. Constitutes of a gas sensor**

Parts	Materials
1 Gas sensing layer	SnO <sub>2</sub>
2 Electrode	Au
3 Electrode line	Pt
4 Heater coil	Ni-Cr alloy
5 Tubular ceramic	Al <sub>2</sub> O <sub>3</sub>
6 Anti-explosion network	Stainless steel gauze (SUS313 100-mesh)
7 Clamp ring	Bakelite
8 Tube pin	Copper plating Ni

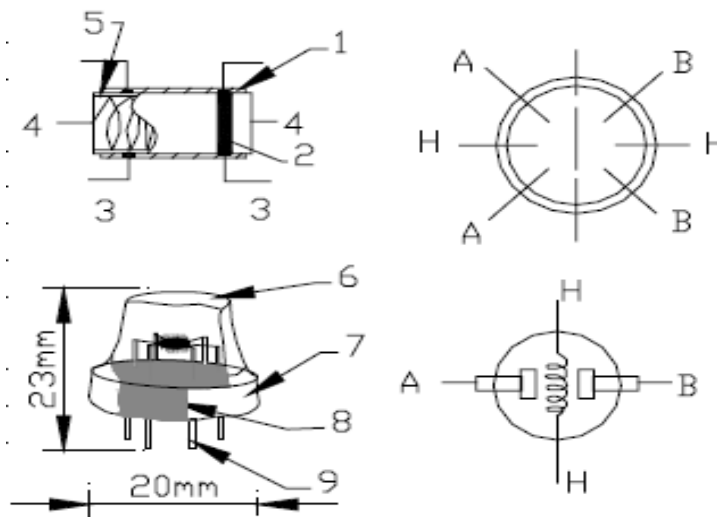


**Fig. 3. MQ gas sensors structure**

**2.3 Mathematical Model of the Sensors**

Depending on the type of sensor, the manufacturer has provided a standard catalog of correlation curves that was used.

$$\text{Curves } \log\left(\frac{R_s}{R_0}\right) = f([C]_{(ppm)})$$

are plotted on a logarithmic scale and are linear. By changing variables

$$Y = \log\left(\frac{R_s}{R_0}\right) \text{ and } X = \log([C]_{(ppm)}), \text{ these equation becomes: } Y = A * X + B.$$

Using the coordinates of two points

$$(X_1, Y_1) \text{ and } (X_2, Y_2),$$

We get A and B:

$$A = \frac{Y_1 - Y_2}{X_1 - X_2} \text{ and } B = Y_2 - \left(\frac{Y_1 - Y_2}{X_1 - X_2}\right) * X_2$$

Subsequently, we will use the calibration curves provided in the technical datasheets to determine the coefficients A and B for each sensor according to the type of gas to be detected.

As said by Priyanka Kakoty and Manabendra Bhuyan: "SnO<sub>2</sub> based MOS gas sensors are most popular for sensing a wide range of gases. Selection of a gas sensing material is crucial due to the fact that selectivity is an important characteristic for designing efficient gas sensing devices" [20]. Therefore, the appropriate sensor for each gas will be selected in paragraphs below according to gas that will be sensed.

### 2.3.1 Dihydrogen and derivatives

These gases were detected by the MQ8 sensor.

As can be seen on Fig. 4. the sensitivity of MQ-8 sensor varies depending on the gas it detects. Hydrogen has the highest variation slope, then come alcohol with a smaller slop variation. Liquefied Petroleum Gas, methane carbon monoxide has very small variation slopes, similar to that of the air. Therefore, we used MQ-8 for measuring hydrogen concentration in flue gas.

In Table 2, calculated the parameters A and B for hydrogen presented.

### 2.3.2 Dihydrogen carbon monoxide and others

These gases were detected with MQ-7 sensor with sensitivity characteristics reported on Fig. 5. It can be seen there that hydrogen has the highest slop variation followed by carbon monoxide. Furthermore, the two curves were almost parallels. Therefore, in the case of gasification where carbon monoxide and hydrogen are the main components, ways should be found to determine separate concentration of either hydrogen or carbon monoxide and deduce concentration of the other.

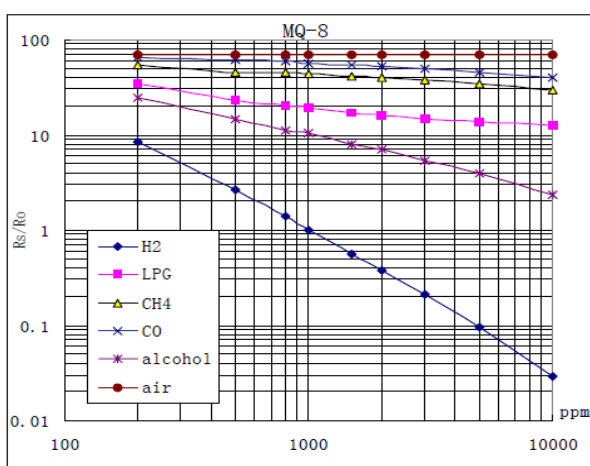


Fig. 4. MQ-8 sensitivity to different gases

Table 2. Calculated values of A and B for MQ-8

Name of Gas	$Y = \log (RS/RO)$	$X = \log (ppm)$	A	B
AIR	70	100	0	1,845
CO	70	1000	A	B
	$Y = \log (RS/RO)$	$X = \log (ppm)$		
	50	3000		
CH4	40	10000	A	B
	$Y = \log (RS/RO)$	$X = \log (ppm)$		
	40	2000		
LPG	30	10000	A	B
	$Y = \log (RS/RO)$	$X = \log (ppm)$		
	20	800		
ALCOL	15	5000	A	B
	$Y = \log (RS/RO)$	$X = \log (ppm)$		
	4	5000		
H <sub>2</sub>	7	2000	A	B
	$Y = \log (RS/RO)$	$X = \log (ppm)$		
	1	1000		
	0,03	10000		

AIR

$$\log \left( \frac{R_g}{R_o} \right) = 1,8451 \leftrightarrow \frac{R_g}{R_o} = 10^{(1,8451)} = 70$$

H<sub>2</sub>

$$\log \left( \frac{R_g}{R_o} \right) = -1,5228 * \log (x) + 4,5686$$

$$= A * \log (x) + B$$

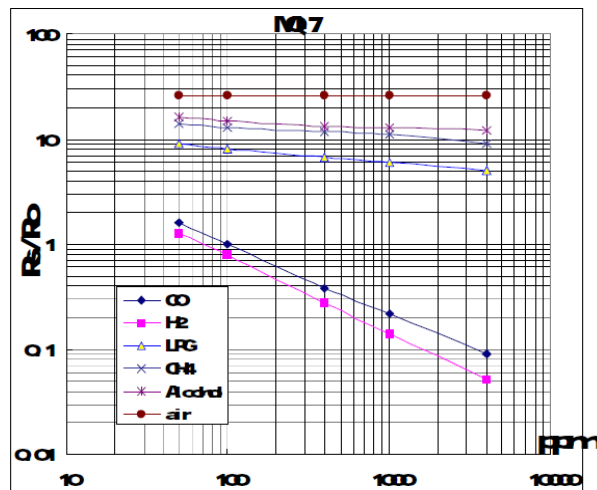


Fig. 5. MQ-7 sensitivity characteristics

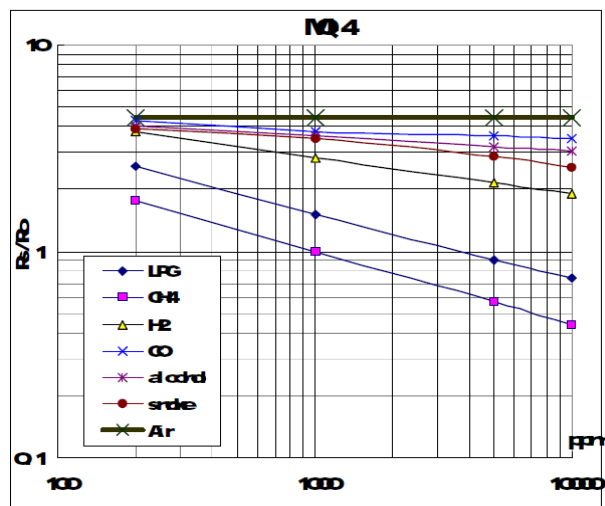


Fig. 6. Sensitivity characteristics of MQ-4

Parameters A and B for MQ-7 are calculated in Table 3: Parameters A and B calculation for MQ-7.

Only equation for CO is given on Table 3. H<sub>2</sub> was calculated from MQ-8 and deduced from MQ-7. For example, if MQ-8 reads a concentration [H<sub>2</sub>] of hydrogen and MQ-7 reads concentration [H<sub>2</sub> + CO], concentration [CO] as MQ-7 reading minus MQ-8 reading was then calculated.

### 2.3.3 Methane and derivatives

These gases were detected with MQ-4 sensor. Sensitivity characteristics of MQ-4 sensor is given on Fig. 6.

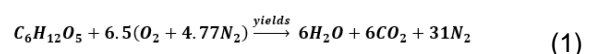
Parameters A and B for MQ-7 are calculated in 4.

As can see, methane has the highest variation slope on MQ-4. It is followed by LPG. We will therefore use this sensor for detecting methane in produced gases.

### 2.3.4 Putting these gases sensors together

In case of gasification, we seek to produce mainly carbon monoxide and hydrogen, plus sometime methane.

The stoichiometric combustion of wood in air containing 21% of oxygen and 79% of nitrogen is the following equation:



When oxygen is not supplied in sufficient quantity, CO is produced in lieu and place of

CO<sub>2</sub>. Also, water vapor is engaged in the so-called water-gas shift reaction that produce hydrogen as a reaction between carbon dioxide and water vapor according equation 2 to:



Consequently, we have mixture of CO, H<sub>2</sub>, CH<sub>4</sub>, CO<sub>2</sub> and N<sub>2</sub> from the gasification of biomass.

Knowing the concentrations of each of these gases thank to MQ sensors will help us monitor the gasification process.

These gases concentration will be calculated with a microcontroller as a computer under the Microchip Integrated Development Environment (IDE) named MPLAB IDE v8.80.

**Table 3. Parameters A and B calculation for MQ-7**

Name of Gas	Y = log (RS/RO)	X = log (ppm)	A	B
AIR	26	50	0	1,4150
	26	4000		
Alcohol	Y = log (RS/RO)	x = log (ppm)	A	B
	17	50	-0,06122	1,3345
	13	4000		
CH4	Y = log (RS/RO)	X = log (ppm)	A	B
	15	50	-0,11657	1,3741
	9	4000		
LPG	Y = log (RS/RO)	x = log (ppm)	A	B
	9	50	-0,13414	1,1821
	5	4000		
CO	Y = log (RS/RO)	x = log (ppm)	A	B
	1	100	-0,65276	1,3055
	0,09	4000		
H2	Y = log (RS/RO)	X = log (ppm)	A	B
	0,8	100	-2,0588	4,0207
	0,02	600		
CO: $\log\left(\frac{R_s}{R_0}\right) = -0,6527 * \log^?(x) + 1,3055 = A * \log^?(x) + B$				

**Table 4. Parameters A and B calculation for MQ-4**

Name of Gas	Y = log (RS/RO)	X = log (ppm)	A	B
AIR	4,5	200	0	0,653212514
	4,5	10000		
co	Y = log (RS/RO)	X = log (ppm)	A	B
	4,3	200	-0,048994451	0,746206157
	3,55	10000		
ALCOL	Y = log (RS/RO)	X = log (ppm)	A	B
	4	200	-0,065156122	0,751986183
	3,1	10000		
SMOKE	Y = log (RS/RO)	X = log (ppm)	A	B
	3,85	200	-0,100347494	0,816363322
	2,6	10000		
H2	Y = log (RS/RO)	X = log (ppm)	A	B
	3	700	-0,176091259	0,978118151
	2	7000		
LPG	Y = log (RS/RO)	X = log (ppm)	A	B
	0,9	5000	-0,325925871	1,159832531
	2,05	400		
CH4	Y = log (RS/RO)	X = log (ppm)	A	B
	1	1000	-0,307227444	0,921682331
	0,55	7000		
CH4: $\log\left(\frac{R_s}{R_0}\right) = -0,3072 * \log^?(x) + 0,921 = A * \log^?(x) + B$				

### 3. RESULTS AND DISCUSSION

#### 3.1 Calibration of the MQ gas Sensors

Calibration of MQ gases sensors mainly consist in the determination of resistance  $R_s$ . For a concentration  $x$  given in ppm, we obtain an electrical resistance  $R_s$  at the sensor output through the following properties:

##### 3.1.1 Mathematical equations for using gas sensors

Through the calibration curves, we know that:

$$\log\left(\frac{R_s}{R_0}\right) = A * \log(x) + B$$

If we note  $x$  the gas concentration in ppm,  $A$  and  $B$  the constants depending on the type of sensor used, the we can deduce:

$$x = 10^{\left(\frac{\log\left(\frac{R_s}{R_0}\right) - B}{A}\right)} \text{ or also}$$

$$\frac{R_s}{R_0} = 10^B * x^A \text{ or also}$$

$$x = \left(\frac{R_s}{R_0} * 10^{-B}\right)^{\frac{1}{A}}$$

We have summarized the values obtained for  $A$  and  $B$  in the two Table 4 and Table 5.

Hence the following mathematical functional block in steady state for each sensor:

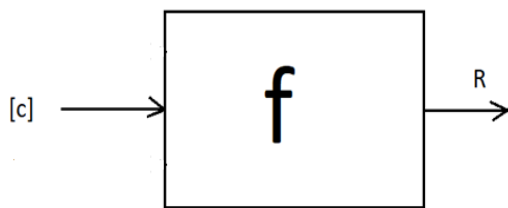


**Fig. 7. Functional bloc of the sensors**

$[C]=x$ : concentration of the inlet gas.  $R=R_s$ : output resistance.

$f$ : the mathematical steady-state input-output correlation function.

##### 3.1.2 Measurement range

The Table 6, Table 7 and Table 8 represent the measurement ranges of the sensors.

**Table 4. Parameter A values of the 3 gas sensors**

MQ4 (CH4)	MQ7 (CO)	MQ8 (H2)
-0,3072	-0,6527	-1,522

**Table 5. Parameter B values of the 3 gas sensors**

MQ4 (CH4)	MQ7 (CO)	MQ8 (H2)
0,921	1,3055	4,5686

**Table 6. H2: MQ8**

X= [C] (ppm)	100	10000
RS (kΩ)	10	60

**Table 7. CO: MQ-7**

X= [C] (ppm)	10	10000
RS (kΩ)	2	20

**Table 8. CH4: MQ-4**

X= [C] (ppm)	100	10000
RS (kΩ)	10	60

##### 3.1.3 Intrinsic sensitivity of the sensors

The intrinsic sensitivity of sensors for a variation  $\Delta R$  of the output, can be estimated through the input variation  $\Delta x$ .

It is equal to:

$$\frac{\partial x}{\partial R_s} = \frac{1}{A} * \left(\frac{10^{-B}}{R_0}\right) * \left(\frac{R_s}{R_0} * 10^{-B}\right)^{\left(\frac{1-A}{A}\right)}$$

##### 3.1.4 Implementation in MPLAB IDE

MPLAB IDE is written in C language. Equation from different sensors were derived for each sensor and we obtained results summarized below.



**Fig. 8. Microchip MPLAB IDE logo**



As we can see on Fig. 9, the main program is subdivided in six routines that do a given work. The most important of these is "gaz\_processing ( )" that calculate the different concentrations of the gases as illustrated on Fig. 10.

### 3.2 Electronic Prototype

From the electronic diagrams, we were able to create some prototype power supply and conditioning boards (and). The measurement cards are made with Pic-kit cards from Microchip and Arduino uno. The measurement system was fabricated with prototyping board and assembled together. The power supply board provides 5V, +8V and -8V voltages to the sensors and measurement amplifiers as seen:

### 3.3 Tests Results

On September 23, 2023, gasification measurement tests were carried out and obtained CH<sub>4</sub> concentration values = 310 ppm; CH<sub>4</sub>=10ppm; RH= 72%. Fig. 13 represents a

local display on an LCD screen of the gasification parameters obtained during the test.

These values were lesser than those we go from previous experiments in nearly similar experimental conditions: waste weigh, weather, etc.

These measurement results show low production of combustible gas. The air-dried wood used did not seem to have any problems and it had not rained in the 2 days preceding our handling. At that time, the oxygen concentration measurement module was not yet ready and we did not understand the reason for the failure of our manipulation. On November 1, 2023 at 5 p.m., we then took measurements of the humidity level of the ambient air. There we found 51%. On January 10, 2024, the indicated humidity level was 8%. We then looked for the causes of these differences in values and consulted the history of the weather in Koudougou. So, for September 23, 2023, the following screenshot shows that the weather forecast indicated between 65 and 75% air humidity:

```
void main(void) // main fonction
{
    init_uc(); //microcontroleur initialisation

    while(1) // loop
    {
        // mesurment of gas contration
        if(gaz_process==1)
        {
            gaz_process=0;
            acquisition ();
            integration(0);
            gaz_processing (0);
            integration(1);
            gaz_processing (1);
        }

        // measurement of humidity
        if(fin_hum)
        {
            fin_hum=0;
            humidity_processing ();
        }
    }
}
```

Fig. 9. The main bloc of our program

```
void gaz_processing (int8 canal_in)
// gas concentrartion measurement fonction
{
    float yy, xx,m, b0;
    int16 reste;
    // computing of correction coefficients
    // according to humidity
    k_rh_mq4= (val_humidity /-322.6)+ 1.10;
    k_rh_mq7= (val_humidity/-370.4)+ 1.09;
    if(canal_in==0)
    {
        k_r=1.1560; //k_r= r1_mq7/r0_mq7;
        //k_g=0.889024;

        k_t_mq7=0.9408; //à 34 degré celcius
        k_g= k_t_mq7 * k_rh_mq7;
        m=1.0/a_mq7;
        b0=20.2069143 ;//b0= pow(10,b_mq7);
        vs=vs_mq7;
    }

    if(canal_in==1)
    {
        k_r=1.1599; //k_r= r1_mq4/r0_mq4;
        //k_g=0.887494;

        k_t_mq4=0.9578;
        k_g= k_t_mq4 * k_rh_mq4;
        m=-3.25520833;//m=1.0/a_mq4;
        b0=8.33681185 ;//b0= pow(10,b_mq7);
        vs=vs_mq4;
    }
}
```

Fig. 10. The gases concentrations calculation function of the program

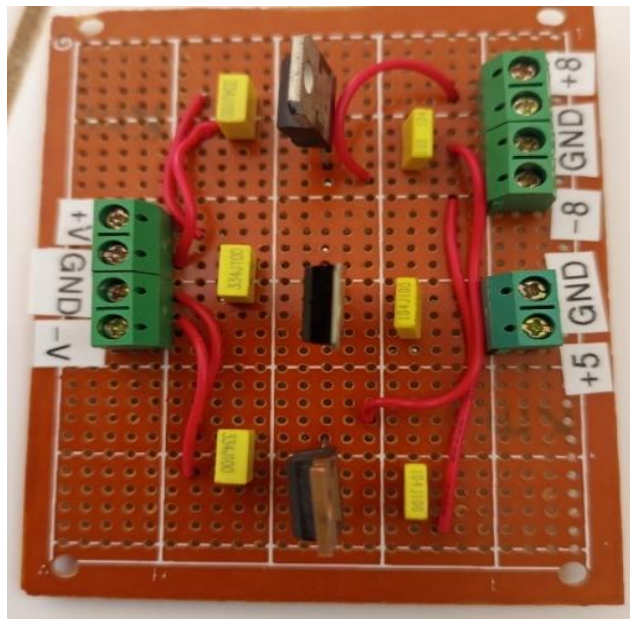


Fig. 11. Main power module

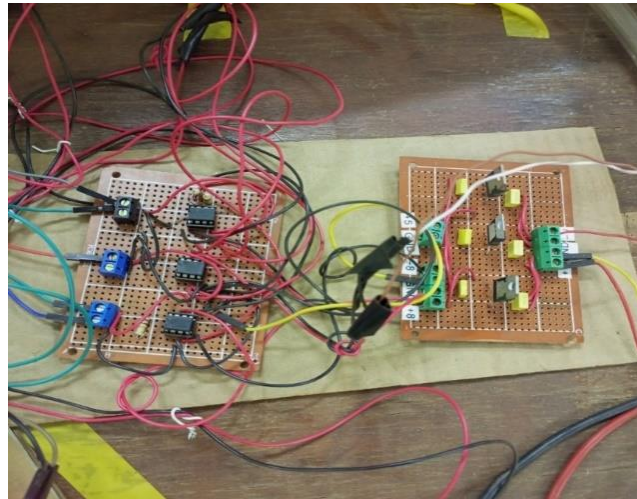
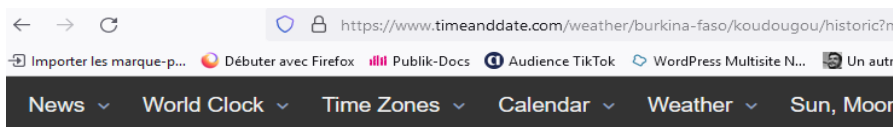


Fig. 12. Treatment and power supply boards



Fig. 13. Test results on LCD display



### High & Low Weather Summary for septembre 2023

	Temperature	Humidity	Pressure
<b>High</b>	36 °C (11 sep, 14 h 00)	100% (1 sep, 02 h 00)	1016 mbar (1 sep, 02 h 00)
<b>Low</b>	22 °C (2 sep, 19 h 00)	47% (30 sep, 13 h 00)	1007 mbar (12 sep, 17 h 00)
<b>Average</b>	29 °C	78%	1012 mbar

\* Reported 1 sep 02 h 00 — 30 sep 23 h 00, Koudougou. Weather by CustomWeather, © 2024

Note: Actual official high and low records may vary slightly from our data, if they occurred in-between our weather recording intervals... [More about our weather records](#)

Fig. 14. Weather in Koudougou during September 2023

Conclusion therefore made that our gas measurement system is working as intended.

#### 4. CONCLUSION

Through this study, the operation of gas concentration sensors made by Hanwey Corp was highlighted. The test body of these sensors is a layer of tin dioxide ( $\text{SnO}_2$ ) whose resistivity is sensitive to contact gases and varies according to their concentration. The electrical model of these sensors is a resistance  $R$  whose measurand is the concentration  $x$  of the gas in contact of the sensor. There is a relation of the form:  $\log(R/R_0) = A \log(x) + B$ , with  $A = -0.3072$ ,  $B = 0.921$  for methane,  $A = -0.6527$ ,  $B = 1.3055$  for carbon dioxide and  $A = -1.522$ ,  $B = 4.5686$  for hydrogen. CO concentration of 310 ppm and  $\text{CH}_4$  concentration of 10ppm was measured. The same method was applicable for  $\text{H}_2$ . However, these sensors were are sensitive to the temperature and humidity of the gases measured. These auxiliary parameters will be investigated in order to find the real physical and mathematical model allowing judicious exploitation of these sensors. Also, except for hydrogen with MQ-8, sensor selectivity is not very good. In case of gasification, MQ7 would indifferently measure hydrogen and carbon monoxide concentration.

#### COMPETING INTERESTS

Authors have declared that no competing interests exist.

#### REFERENCES

1. Joan Nyika, Adeolu Adesoji Adediran, Adeniyi Olayanju, Olanrewaju Seun Adesina and Francis Odikpo Edoziuno, The Potential of Biomass in Africa and the Debate on its Carbon Neutrality, Biotechnological Applications of Biomass; 2016.  
DOI: 10.5772/intechopen.93615, 2020
2. Sustainable Energy for All, [Burkina Faso]: Rapid assessment and gap analysis. 2023;1-2.  
Available:https://www.seforall.org/sites/default/files/Burkina\_Faso\_RAGA\_FR\_Release.pdf,  
Accessed on:26 septembre 2023. French.
3. Nzihou Jean Fidele, Hamidou Salou, Imbga Kossi, Segda Bila Gerard, Ouattara Frederic, Tiemtore Hamadou, Electrical Power Generation from Heat Recovered at the throat of a Downdraft Biomass Gasifier, American Journal of Science, Engineering and Technology. 2023;8(3): 133-140.  
Available:http://www.sciencepublishinggroup.com/j/ajset ISSN: 2578-8345 (Print); ISSN: 2578-8353 (Online)  
DOI: 10.11648/j.ajset.20230803.12, 2023
4. Nzihou Jean Fidele, Hamidou Salou, Segda Bila Gerard, Ouattara Frederic and Compaore Hamidou, Effects of a Cyclone Dimensions on Quality of Syngas Produced with a Wood-fired Biomass Gasifier, Journal of Energy Research and Reviews, Article number JENRR.107030. 2023;15(3):1-14.  
ISSN: 2581-8368
5. Reed TB, Das A, Handbook of Biomass Downdraft Gasifier Engine Systems, Solar Energy Research Institute; 1950.  
Available:https://www.nrel.gov/docs/legosti/old/3022.pdf,  
Accessed on: 15 September 2023.
6. Akhator PE, Obanor AI, Sadjere EG, Design and development of a small-scale biomass downdraft gasifier, Nigerian Journal of Technology (NIJOTECH). 2019; 38(4):922–930.  
Available:http://dx.doi.org/10.4314/njt.v38i4.15  
ISSN: 0331-8443, Electronic ISSN: 2467-8821
7. Mukunda HS, Dasappa S, Paul PJ, Rajan NKS, Shrinivasa U., Gasifiers and combustors for biomass - technology and field studies, Energy for Sustainable Development. 1994;1(3):27-38.
8. Abubakar A. Bukar, M. Ben Oumarou, Babagana M. Tela, Abubakar M. Eljummah assessment of biomass gasification: A Review of Basic Design Considerations, American Journal of Energy Research. 2019;7(1):1-14.
9. Chawdhury MA, Mahkamovb K. Development of a small downdraft biomass gasifier for developing countries. Journal of Scientific Research J. Sci. Res. 2011;3(1): 51-64.  
Available:www.banglajol.info/index.php/JSR
10. Yulin Kong, Yuxiu Li, Xiuxiu Cui, Linfeng Su, Dian Ma, Tingrun Lai, Lijia Yao, Xuechun Xiao, Yude Wang,  $\text{SnO}_2$  nanostructured materials used as gas sensors for the detection of hazardous and flammable gases: A review, Nano Materials Science. 2022;4(4):339-350.

- Available:<https://doi.org/10.1016/j.nanoms.2021.05.006>. 2022  
ISSN 2589-9651
11. Kadek I NuaryTrisnawan, Agung Nugroho Jati, Novera Istiqomah, Isro Wasisto, Detection of Gas Leaks Using The MQ-2 Gas Sensor on the Autonomous Mobile Sensor; 2019.
  12. Nisal Kobbekaduwa, Pahan Oruthota and W.R. de Mel, Calibration and implementation of heat cycle requirement of MQ-7 Semiconductor Sensor for Detection of Carbon Monoxide Concentrations, *Advances in Technology*. 2021;1(2):377-392.
  13. Sohibun I Daruwati, RG Hatika and D Mardiansyah, MQ-2 Gas Sensor using Micro Controller Arduino Uno for LPG Leakage with Short Message Service as a Media Information, *URICSE 2021, Journal of Physics: Conference Series*, 012068 IOP Publishing; 2021.  
DOI: 10.1088/1742-6596/2049/1/012068
  14. Abubakar Yakub Nasir, Bature UI, Tahir NM, Babawuro AY, Adoyi Boniface Hassan AM. Arduino based gas leakage control and temperature monitoring system, *International Journal of Informatics and Communication Technology (IJ-ICT)*. 2020; 9(3):171-178.  
DOI: 10.11591/ijict.v9i3  
ISSN: 2252-8776  
Available:<http://ijict.iaescore.com>, 2020
  15. Huan Hui Yan, Yusnita Rahayu, Design and development of gas leakage monitoring system using Arduino and ZigBee, *Proceeding of International Conference on Electrical Engineering, Computer Science and Informatics (EECSI 2014)*, Yogyakarta, Indonesia. 2014:20-21.
  16. Dewi L, Somantri Y. Wireless sensor network on lpg gas leak detection and automatic gas regulator system using Arduino, *IOP Conf. Serie: Material Sciences Engineering*, 384 012064; 2018.
  17. Laghrib Souad, Synthesis of Thin Films of: SnO<sub>2</sub>, SnO<sub>2</sub>: In by Two Physical and Chemical Processes and Study of Their Characterization, PhD Thesis, Ferhat Abbas University, Algeria, French. 2018:139.
  18. Jacquemin J. Optical Properties of Intrinsic SnO<sub>2</sub> AND  $\beta$ -PbO<sub>2</sub> neighborhood of the gap. *Journal de Physique Colloques*. 1974 ;35 (C3):C3-255-C3-260.  
DOI: 10.1051/jphyscol:1974337. jpa-00215585
  19. Laghrib Souad, Hania Amardjia-Adnani, Dahir Abdi, Jean-Marc Pelletier, Development and study of thin layers of SnO<sub>2</sub> obtained by evaporation under vacuum and annealed under oxygen, *Revue des Energies Renouvelables* 10 N°3 French.2007:357–366.
  20. Priyanka Kakoty, Manabendra Bhuyan, SnO<sub>2</sub> based gas sensors: Why it is so popular?

© 2024 Zoundi et al.; This is an Open Access article distributed under the terms of the Creative Commons Attribution License (<http://creativecommons.org/licenses/by/4.0>), which permits unrestricted use, distribution, and reproduction in any medium, provided the original work is properly cited.

Peer-review history:

The peer review history for this paper can be accessed here:  
<https://www.sdiarticle5.com/review-history/112774>